

Numerical Analysis of Microfluidic Magnetic Bead Separation Utilizing an Integrated Array of Magnetic Elements Magnetized by a Homogenous Bias Field

Saud A. Khashan¹ and Edward P. Furlani^{2,3}

Mechanical Engineering Department¹, United Arab Emirates University, Al-Ain, UAE

Dept. of Electrical Engineering², Dept. Chemical & Biological Engineering³,
University at Buffalo (SUNY), Buffalo, NY 14260-4200, efurlani@buffalo.edu

ABSTRACT

An analysis is presented of magnetic bead separation in a microfluidic system with integrated magnetic functionality. The system consists of a flow cell on a substrate that contains an embedded array of passive soft-magnetic elements. The elements become magnetized in the presence of an applied field and produce a force that separates the beads from the flow as that pass through the microchannel. In this paper, bead capture is analyzed using a model that combines numerical transport analysis with closed-form field analysis. Particle and fluid transport are predicted using computational fluid dynamics (CFD), while the magnetic force that governs bead capture is obtained in closed-form. The CFD analysis takes into account coupled two-way momentum transfer between the beads and the fluid and the model is used to quantify the impact of this coupling on both the capture efficiency and distortions of flow velocity field. The model is demonstrated via application to a microfluidic system, and the analysis demonstrates that it predicts important aspects of bead transport and separation that are not observed using more conventional one-way coupling analysis, especially for applications involving high particle loading and/or low flow rates. The model presented here is computationally much more efficient and accurate than purely numerical models and should prove useful for the rational design and optimization of numerous magnetic particle-based microfluidic applications, examples of which are also discussed.

Keywords: Magnetic separation, particle-fluid coupling, magnetophoresis, magnetophoretic microsystem, magnetic particle transport, field-directed particle transport.

1 INTRODUCTION

Magnetic particles (beads) are increasingly used in microfluidic systems to selectively separate and sort biomaterial for a broad range of biomedical and clinical diagnostic applications [1]. Magnetic beads are well suited for such applications because they can be functionalized to selectively bind to (label) target biomaterials such as proteins, enzymes, nucleic acids or whole cells, thereby

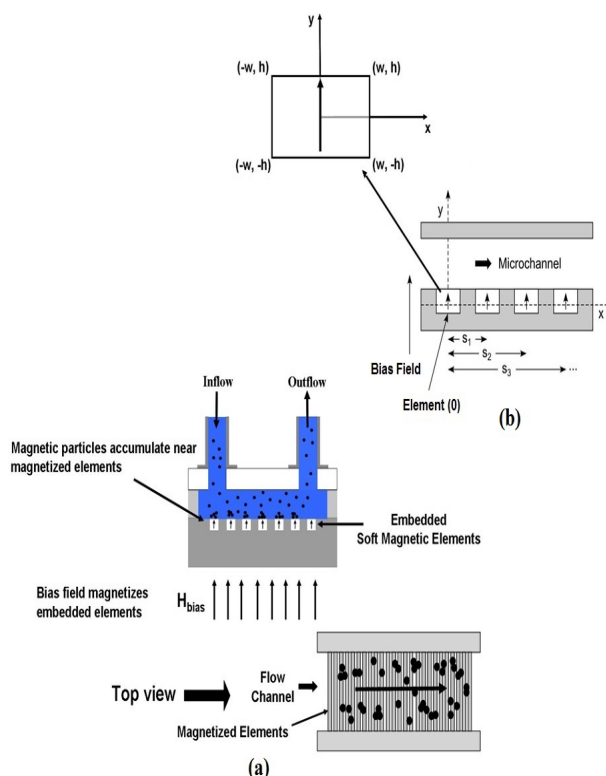


Figure 1. Passive magnetophoretic system: a microfluidic flow cell on a substrate containing an array of soft-magnetic elements.

enabling manipulation of such materials in microfluidic systems using an external field. An example of such a system is shown in Fig. 1. This system consists of a flow cell integrated with a substrate that contains an embedded array of passive soft-magnetic (e.g. Ni) elements. The elements become magnetized in the presence of an applied field and produce a force that separates the beads from the flow as that pass through the microchannel. Significantly, this force can be switched on and off by applying and removing the bias field, and no electrical energy source is required to effect separation.

To date, to vast majority of the theoretical models used to predict magnetic field-induced particle transport and separation for such systems have been limited to one-way

particle-fluid coupling in which the flow field is uncoupled from particle motion, i.e. the particle motion does not impact fluid flow. However, such coupling can have a significant impact on system performance and needs to be taken into account for rigorous design and optimization. In this article we introduce a fully-coupled model that is computationally efficient and well-suited for the optimization of novel magnetophoretic microsystems prior to fabrication..

2 THEORY AND MODELING

The motion of colloidal magnetic particles under the influence of an applied field is governed by several factors including the magnetic force, fluidic drag, particle-fluid coupling, Brownian motion and interparticle effects such as magnetic dipole-dipole interactions [1-4]. A complete analysis of this process is highly complex and beyond the scope of this study. In this paper, the dominant magnetic and fluidic forces are taken into account as well as two-way particle-fluid coupling. The particle size and concentration are such that the effects of Brownian motion and interparticle interactions can be neglected.

We use a combined Lagrangian-Eulerian CFD-based approach to model fully-coupled particle-fluid transport interactions [3-6]. The Lagrangian analysis is used to track the motion of individual particles, and the particle motion is coupled to the fluid by introducing a particle force sink into the Navier-Stokes momentum equations, which are solved using an Eulerian-based CFD analysis. In the Lagrangian formulation particle transport is governed by Newton's second law,

$$m_p \frac{d\mathbf{u}_p}{dt} = \sum \mathbf{F}_{ext} \quad (1)$$

where m_p and \mathbf{u}_p are the mass and the velocity of the particle and

$$\sum \mathbf{F}_{ext} = 6\pi\eta a(\mathbf{u} - \mathbf{u}_p) + V_p(\rho_p - \rho)\mathbf{g} + \mathbf{F}_m \quad (2)$$

is the sum of the external forces on the particle. The variables \mathbf{u} , ρ and η are the velocity, density and viscosity of the carrier fluid, ρ_p , a and V_p are the density, radius and volume of the particle, and \mathbf{g} is the gravitational acceleration. The first term on the right hand side represents the drag as described by Stokes' law and the second term is the lift (buoyant) force. The third term is the magnetic force, which is predicted using an "effective" dipole moment approach where the magnetized particle is replaced by an "equivalent" point dipole. The force on the dipole (and hence on the particle) is given is given by :

$$\mathbf{F}_m = \mu_o (\mathbf{m}_{p,eff} \cdot \nabla) \mathbf{H}_a, \quad (3)$$

where μ_f is the permeability of the transport fluid and $\mathbf{m}_{p,eff}$ is the "effective" dipole moment of the particle. \mathbf{H}_a is the applied magnetic field intensity (A/m) at the center of the particle, were the equivalent point dipole is located. If the particle has a magnetization \mathbf{M}_p , then $\mathbf{m}_{p,eff} = V_p \mathbf{M}_p$. The magnetization is assumed to be a linear function of the field intensity up to saturation after which it remains a constant with a value of \mathbf{M}_s . The force can be written as [2,5],

$$\mathbf{F}_m = \mu_o V_p f(H_a) (\mathbf{H}_a \cdot \nabla) \mathbf{H}_a, \quad (4)$$

where

$$f(H_a) = \begin{cases} \frac{3(\chi_p - \chi_f)}{(\chi_p - \chi_f) + 3}, & H_a < \frac{(\chi_p - \chi_f) + 3}{3(\chi_p - \chi_f)} M_s, \\ M_s / H_a, & H_a \geq \frac{(\chi_p - \chi_f) + 3}{3(\chi_p - \chi_f)} M_s \end{cases} \quad (5)$$

Taking this into account, Eq. (1) can be rewritten as

$$\frac{d\mathbf{u}_p}{dt} = \tau^{-1} (\mathbf{u} - \mathbf{u}_p) + \mathbf{A} \quad (6)$$

where

$$\mathbf{A} = \frac{V_p(\rho_p - \rho)\mathbf{g} + \mu_f V_p f(H_a) \mathbf{H}_a \cdot \nabla \mathbf{H}_a}{m_p} \quad (7)$$

The characteristic relaxation time $\tau = m_p b$ is the time required for a particle to respond to changes in fluid motion. The trajectory of a particle is predicted using

$$\frac{d\mathbf{x}_p}{dt} = \mathbf{u}_p. \quad (8)$$

The equations of motion (6) and (8) can be integrated using numerical techniques such as the fourth-order Runge-Kutta method, which we use for our analysis.

We use an Eulerian approach to model the flow of the incompressible carrier fluid, which is governed by the equations,

$$\nabla \cdot \mathbf{u} = 0, \quad (9)$$

$$\rho \left(\frac{\partial \mathbf{u}}{\partial t} + \mathbf{u} \nabla \mathbf{u} \right) = -\nabla P + \nabla \cdot (\eta \nabla \mathbf{u}) - \mathbf{f}_p. \quad (10)$$

We assume that the particle volume fraction (i.e. particle loading) is sufficiently low so that its effect on fluidic continuity and on the inertia and stress flux terms in the Navier-Stokes equations can be neglected. The term \mathbf{f}_p in these equations is a force density that accounts for the counter drag force exerted by the particles on the fluid.

Two-way particle-fluid coupling is modeled by including a particle-weighted sink term \mathbf{f}_p in the Navier-Stokes Eq. (10). This force density represents the counter drag force exerted by the particles (located in the continuum cells) on the fluid. We use the discrete phase model (DPM) in the ANSYS FLUENT program (www.ANSYS.com) to implement the two-way particle-fluid coupling. The DPM is based on a combined Euler-Lagrange approach wherein the Navier-Stokes equations are solved within an Eulerian framework, while the dispersed phase is modeled using a Lagrangian formalism that tracks the trajectories of particle parcels, each containing particles with the same properties (i.e. diameter, velocity, and initial conditions). Specifically, in the standard DPM, each particle represents a parcel of particles and the behavior of each parcel is determined by the behavior of its constituent particles. In our study, a parcel is subjected to a magnetic force, fluidic drag and gravity. The magnetic force is predicted using a closed-form expression, which is compiled in the FLUENT program using a User Defined Function (UDF) [3,4]. The particle-fluid momentum transfer is computed using

$$-\mathbf{f}_p = \frac{1}{m_p} \sum_p \frac{1}{b} (\mathbf{u}_p - \mathbf{u}_f) \dot{m}_p \Delta t. \quad (11)$$

This force density is equal but opposite to the force that the fluid exerts on the particles. The summation is taken over all parcels that reside in the computational cell. The variables \dot{m}_p and Δt are the mass flow rate of each parcel, and the residence time that a parcel spends in the computational cell, respectively. The continuum flow velocity is interpolated to the moving parcel position within the cell.

3 RESULTS

We use the model to study bead separation in a microfluidic system shown in Fig. 1. We assume that the system has 5 soft-magnetic permalloy elements (78% Ni 22% Fe, $M_{es} = 8.6 \times 10^5$ A/m) that are embedded immediately beneath the microchannel. Each element is 100 μm high, 100 μm wide, and they are spaced 50 μm apart edge to edge ($w = h = 50$ μm in Fig. 1b). A bias field of $H_{bias} = 3.9 \times 10^5$ A/m ($B = 5000$ Gauss) is sufficient to saturate the elements [3]. The microchannel is taken to be 200 μm high, 2 mm wide, and 10 mm long, which justifies the use of a 2D fluidic analysis. Incompressible Newtonian fluid (water) enters the microchannel at the inlet (left end) as fully developed laminar flow with an average velocity u_{in} . The outlet pressure is set to zero. The MyOne™ beads produced by Dynal Biotech (www.dynabead.com) are used for the analysis [3].

The magnetic field and force analysis is performed using analytical closed-form analysis as described in

references [2, 3]. Surface plots of the horizontal and vertical magnetic force components F_{mx} and F_{my} for the present system are shown in Figs. 2a and b, respectively. These are computed over a region above the substrate that extends from 0-100 μm above the elements and from -100 μm to the left of the array to +100 μm to the right of the array. As shown in Fig. 2a, the horizontal force component F_{mx} peaks near the edges of an element ($x = \pm w$) and alternate in direction (+ or forward, to - or backward) from the left-hand (leading) to the right-hand (trailing) edge of the element. This implies that as a particle moves from the inlet to the outlet, left to right above an element, it experiences a forward horizontal acceleration (+, positive force) as it passes the leading edge, followed by a deceleration (-, negative force) as it passes the trailing edge. This, combined with the effects of the vertical magnetic force component determines the residence time and trapping site at the base of the microchannel.

The profile of the vertical force component F_{my} is shown in Fig. 2 b. Close to the elements F_{my} exhibits dual minima near the edges of an element, which represent an attractive force at these positions. However, farther away a single minimum occurs at the center of the element. One of the most interesting features of the F_{my} profile is that it alternates in polarity (direction) across an element. Specifically, F_{my} is upward (repulsive) just to the left of an

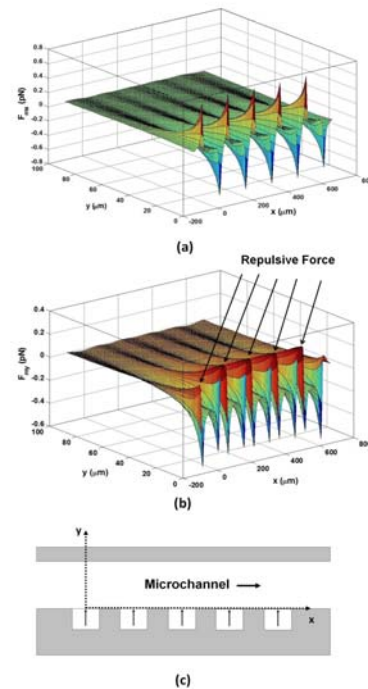


Figure 2. Magnetic force above five soft-magnetic elements: surface plots of (a) F_{mx} , (b) F_{my} .

element, downward (attractive) directly above an element, and upward (repulsive) just to the right of an element. Moreover, the repulsive force is stronger and more extended above the gaps between elements. This behavior is due to the combined effects of the bias field and the field of the magnetized elements. The bias field tends to impose an upward magnetization in the particle throughout its range of motion, whereas the magnetized elements produce a field gradient that changes in both magnitude and direction point-wise within the microchannel. This gives rise to a spatially varying force on the particle that is attractive in some regions and repulsive in others. The alternating nature of this force profile has significant implications for particle motion and capture efficiency. As a particle moves from the inlet to the outlet, left to right across an element, it first accelerates upward near the leading edge, then downward above the element, and then upward again as it passes the element. Thus, the particle exhibits oscillatory motion as it moves through the microsystem as shown. This can potentially be used to effect the mixing of constituent fluids in a multiphase system.

Particle-fluid transport is studied using both one-way and two-way particle-fluid coupling analysis. A parametric analysis of capture efficiency (CE) vs. particle volume fraction ϕ at the inlet is performed for an inlet velocity of $u_{ave} = 3$ mm/s. The particles are released in 100 distinct streams that are uniformly distributed along the height of the inlet. Predicted flow streamlines and particle trajectories along with CE and are shown in Figs. 3. The particle trajectory profiles in blue are superimposed with red bands that are used to visualize the portions of the flow that are directly above the elements, i.e. the left and right hand edges of the red bands are aligned with the corresponding edges of the magnetic elements, which are located beneath the microchannel outside the computational domain. Note that in one way coupling (Fig. 3a) the streamlines are horizontal, which means that they are parallel to the undistorted laminar velocity field. However, in two-way coupling (Fig. 3 b-f), the streamlines can become distorted (nonparallel) indicating that particle-fluid coupling has altered the flow, even to the extent of creating regions of circulating fluid (vortex). The performance criterion for magnetic separation is defined in terms of the capture efficiency,

$$CE = \frac{\text{number of particles captured}}{\text{total number of particles}} \quad (12)$$

The two-way coupling analysis shows that there is a cooperative effect between the magnetic force and particle-induced flow towards capture regions that enhances capture efficiency

4 CONCLUSIONS

A model has been presented that predicts magnetic bead separation in microfluidic systems with magnetic functionality in the form of an array of magnetic elements.

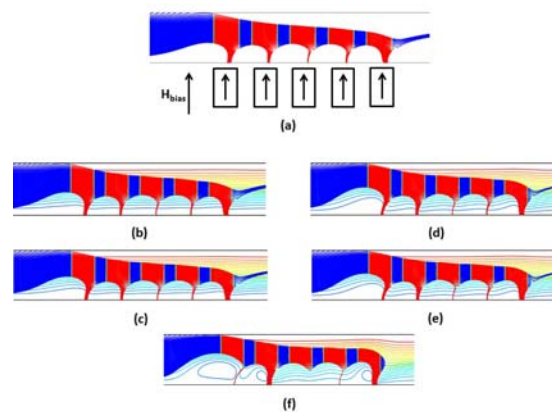


Figure 3. Analysis showing streamlines and particle trajectories: (a) one-way coupling, CE=68%, (b)-(f) two-way coupling, (b) $\phi_{in}=0.00556\%$, CE = 69%, (c) $\phi_{in}=0.0092\%$, CE = 70%, (d) $\phi_{in}=0.0185\%$, CE = 72%, (e) $\phi_{in}=0.0278\%$, CE = 74%, (f) $\phi_{in}=0.0463\%$, CE = 75%.

The model combines numerical transport analysis with closed-form field analysis and accounts for two-way particle-fluid coupling. It is computationally efficient and predicts many critical aspects of system performance that cannot be predicted using one-way coupling analysis. One such feature is a cooperative magnetic force-flow effect that enhances capture efficiency. The model is well-suited for parametric analysis and should prove useful for the design and optimization of novel magnetophoretic microsystems.

Acknowledgments The first author acknowledges the financial support received from the Research Affairs at the UAE University under contract number 01-05-7-12/10.

REFERENCES

- [1] E. P. Furlani, Magnetic Biotransport: Analysis and Applications, *Materials*, 3(4): 2412-2446, 2010.
- [2] E. P. Furlani, Analysis of Particle Transport in Magnetophoretic Microsystem, *J. Appl. Phys.* 99 (2): 024912, 2006.
- [3] S. A. Khashan and E. P. Furlani, Coupled particle-fluid transport and magnetic separation in microfluidic systems with passive magnetic functionality, *J. Phys. D, Appl. Phys.* 46 (12) 125002 doi:10.1088/0022-3727/46/12/125002, 2013.
- [4] S. A. Khashan and E. P. Furlani, Effects of Particle-fluid Coupling on Particle Transport and Capture in a Magnetophoretic Microsystem, *Microfluidics and Nanofluidics*, 12 (1-4), 565-580, 2012.
- [5] E. P. Furlani and X. Xue, Field, force and transport analysis for magnetic particle-based gene delivery, *Microfluidics and Nanofluidics*, DOI 10.1007/s10404-012-0975-x, 2012.
- [6] S. A. Khashan, and Y. Haik, Numerical Simulation of Bio-magnetic Fluid Downstream an Eccentric Stenotic Orifice, *Physics of Fluids*, 18 (11), 113601, 2006.